Materials and Structures (2025) 58:240
https://doi.org/10.1617/s11527-025-02763-1

ORIGINAL ARTICLE

Tensile behaviour of four LVL-truss end connections for timber spatial structures

Andrea Fabbri · Fabio Minghini · Nerio Tullini

Received: 6 May 2025 / Revised: 10 July 2025 / Accepted: 29 July 2025

Abstract This study analyzes four types of steel-to-timber connections for potential use in spatial truss structures with high-performance, small-section Laminated Veneer Lumber (LVL) elements. The experiments were comprised of 42 monotonic pull-pull tests, including 30 tests on dowel-type connections and 12 tests on screwed connections. Dowel-type connections were subdivided into dowel-nut connections and bolted connections featuring either one inner or two outer steel plates. None of the dowel-type connections met code requirements on minimum lateral-edge distance. For some configuration, also loaded-end distance was non-conforming. Screwed connections used a threaded insert parallel to the longitudinal element axis, accommodating a metric threaded rod. Even in this case, the connection was non-conforming due to violation of code requirements on edge distance and inclination angle with respect to veneer planes. Bolted connections showed high load-carrying capacities, but at the cost of a significant steel usage. The screwed connection, while reducing steel usage, exhibited high stiffness but relatively small load-carrying capacity. This last one, however, was shown to be improved by the application of transverse confinement. The dowel-nut connection proved to be particularly effective, combining good mechanical performance with a low aesthetic impact. These results provide valuable insights into the design of safe and efficient connections for LVL spatial structures, contributing to the growth of knowledge on sustainable engineering applications.

Keywords Beech LVL · Spatial truss · Dowel-nut · Bolted connection · Dowelled connection · Dowel-type connection · Screwed connection · Threaded insert · Monotonic test · Pull-pull test · Transverse confinement

1 Introduction

In recent decades, sustainable architecture has increasingly focused on wood as a construction material. Timber structures offer significant advantages, including excellent energy performance, reduced environmental impact, and carbon storage, which helps mitigating climate change [1]. Responsible management of forests and end-of-life wood products, with use of biomass for the replacement of fossil fuels, is expected to provide, in the long run, a significant reduction in CO_2 emissions [2].

Opportunities offered by the application of modern prefabrication technologies to timber construction allow obtaining structural shapes unthinkable just a few years ago [3]. Sustainability in whole timber structures may be further improved including usually discarded trees [4, 5]. Also, still relatively little

A. Fabbri · F. Minghini (✉) · N. Tullini
Department of Engineering, University of Ferrara, Ferrara, Italy
e-mail: fabio.minghini@unife.it

Published online: 29 August 2025

used materials with strong potentials such as glubam deserve exploration [6]. Reconfigurable modular solutions have also become possible thanks to robotic fabrication, so promoting recycling and reusing of dimensional timber components [7].

Spatial structural systems made of timber elements arranged in trusses, such as grids [8, 9], provide high efficiency and allow for large spans without intermediate columns. The efficient design of these structures strongly depends on the type of connection used to join the various members to one another.

Connections can be classified into three main categories, i.e., traditional carpentry, metal and glued joints. Each type of connection has its own pros and cons, being common design criteria based on structural and fire performance, construction speed, simplicity, aesthetics, and cost. The behaviour of joints belonging to the first category relies on direct contact and friction, and still deserves attention due to the widespread use of these connections in historical construction [10]. These joints are typically suited to plane trussed beams, and are therefore rarely used in three-dimensional frames. In timber structures, timber is preferably used alone whenever possible. When timber alone is insufficient, steel is added. Therefore, the second of the mentioned connection categories, using metal connectors for force transmission, is very common when high performance in terms of load-carrying capacity and/or ductility is required, and may be more easily tailored to timber spatial structures. Joints adopted in three-dimensional grid systems make use of metal connectors arranged in either transverse or longitudinal element direction (see Sect. 1.1 of [11] and references cited therein). Finally, the use of glued joints is increasingly widespread, even though some specific aspects, such as the long-term behaviour of adhesives, still deserves to be investigated. Joints using connectors adhesively bonded in the longitudinal element direction, such as glued-in rods, are characterized by high stiffness and seem then promising for structures unable to accommodate large deformations. However, glued connections are not reversible, and their failure is brittle, which limits their use. Nonetheless, glued-in rods joints are now becoming common in timber structures. When dealing with glued-in rods in Cross Laminated Timber (CLT), the relatively high scatter in the experimental load-carrying capacity makes available design equations not appropriate [12], so requiring further research efforts. Moreover, the assembling operations of spatial structures with this type of connection may require complex construction details.

Among the joints with metal connectors in the transverse element direction, dowel-type connections are the most common in timber structures [3]. These connections are often preferred due to their ease of implementation. The relevant, consolidated design approach for dowel-type connections stated by Eurocode 5 [13], referred to as European or Johansen's Yield Model, is based on the seminal study of Johansen [14], relying upon the assumptions of rigid-plastic behaviour for timber and elastic behaviour for metal connectors. This approach was modified a few years later by Meyer [15], who introduced the hypothesis of plastic connectors. Based on tests on dowel-type connections featuring multiple fasteners loaded parallel to grain, Jorissen [16] provided design equations based on the European Yield Model, which was corrected by a suited fracture mechanics model to take account of possible brittle failures occurring in single-fastener connections. The "group effect", resulting, for multiple-fastener connections, in a smaller capacity compared with that of one single fastener multiplied by the number of connectors (n), was deeply investigated by Jorissen, who defined an effective number of fasteners, $n_{ef} \leq n$, depending on n, fasteners spacing and timber thickness-to-fastener diameter ratio. Although minimum spacing, end and edge distances of connectors required by Eurocode 5 are aimed at obtaining ductile failure [17], the experimental evidence shows that a brittle connection behaviour cannot be excluded at all [18]. The load-carrying capacity seems to be also influenced by usually disregarded effects, such as those due to decrease in moisture content [19] and dowel surface roughness [20]. The need for inclusion of fracture mechanics considerations into design approaches for dowelled connections was highlighted by Quenneville' and Mohammad's researches (see [21, 22] and references cited therein), forming the basis of the current version of Canadian Standard on wood structures [23].

In assembling steel-to-timber dowel-type connections, steel plates allow for simple installation. These plates can be placed either externally or internally, with fire resistance and aesthetic impact influencing this choice. An alternative joint type with similar structural behaviour is the "Dowel-nut" connection [24], comprised of a dowel provided with a threaded

hole orthogonal to its axis, suitable to accommodate a threaded rod (Fig. 1). The dowel is usually obtained from a cylinder of structural steel.

According to the modern principles of architectural design applied to large-span spatial timber structures, the identification of high-performance wood products becomes crucial. An innovative solution is offered by Laminated Veneer Lumber (LVL), which uses 3–4 mm thick, strongly selected laminae, resulting in a reduced impact of defects and superior strengths and stiffnesses compared with traditional wood products [25–27]. A recent sustainability study [28] has also shown that using LVL would reduce both CO_2 emissions and embodied energy compared with Glued Laminated Timber (GLT).

At equivalent structural demands, a LVL element would generally have smaller dimensions than a classical timber element. While this feature provides numerous advantages, it introduces dimensional challenges in connections, where reduced timber sections face strict regulatory limits on minimum edge distances of metal connectors. In analogy with other wood products, even for LVL adequate edge and mutual distances of connectors may ensure a significantly ductile joint response [29]. Conversely, for reduced edge distances the failure mode is dominated by splitting, and the relevant load-carrying capacity may result anything but negligible, even for the case of load applied perpendicular to grain [30]. This aspect will require specific predictive models.

The embedment strength of mixed-species LVL with cross-banded configurations was evaluated in [31]. In [32–34], embedment and connection tests on beech LVL were presented. The former, having the aim of evaluating the embedment strength, were carried out on single-dowel connections. Connection tests were conducted on two-row dowelled connections, including 1, 2 or 6 dowels per row. The fasteners were always oriented orthogonal to the veneer planes. Whilst loaded-end distance, referred to as $a_{3,t}$ in Eurocode 5 [13], was changed to compare configurations meeting standard requirements (i.e., showing $a_{3,t}=7d$, with d dowel diameter) to non-conforming cases with $a_{3,t}=3.5d$ and $5d$, lateral-edge distances always were code-conforming ($=3d$). The tests highlighted brittle failure in the case of absence of cross layers. For 14% and 23% of cross layers, ductile behaviour was generally observed, toghether with an improved embedment strength. As far as the withdrawal strength of screws in LVL is concerned, test results relative to beech-poplar mixed configurations and to three different species such as beech, poplar and hornbeam were presented in [35] and [36], respectively.

Fig. 1 Sectional view of dowel-nut end connection in timber element

1.1 Previous studies on dowel-type connections for LVL spatial structures

In [37] the results obtained from 42 pull-pull tests on dowel-nut connector in beech LVL element, including 22 monotonic and 20 cyclic load tests, were presented. The tested LVL elements had a square cross-section with the side length of 50 mm. In monotonic load tests, the effects due to connector's end distance and orientation with respect to the veneers were investigated. To avoid interaction between timber failure and connector's yielding, class 12.9 steel (nominal yield strength $f_y=1080$ MPa) was used for the 20 mm-diameter dowel-nut. The tests with dowel-nut oriented orthogonally to the veneers led to increased and less scattered load-carrying capacity compared with parallel connectors. The failure modes were invariably brittle. In cyclic load tests, dowel-nuts of grade S355 steel ($f_y=355$ MPa) were also used for comparison, and plastic deformation were observed in connectors for the largest end distances.

To interpret the brittle failure mechanisms, monotonic pull-pull tests on the same connection were also simulated in [38] using a regularized extended finite element method (XFEM). This numerical technique allows describing the crack path by specific enrichment functions, independently of the standard finite element mesh geometry.

In trusses, usually comprised of struts and ties (which sometimes may also be subjected to load inversion), an efficient behaviour in both tension and compression is required. To make the response in compression more efficient, the application of an initial tightening torque to the dowel-nut connection was proposed and tested in [37] on individual LVL

elements. The same technology has proved in [11] to yield a decisive improvement to the behaviour of entire LVL spatial structures. Preloading the connection enables the direct transfer of compressive load to the timber element. Therefore, the slender axial threaded rod screwed into the dowel-nut turns out to be not overloaded, and load-carrying capacity of timber struts results maximized. The failure in compression will be ruled by strut buckling.

2 Research objectives

The objective of this research is to test and compare the mechanical performance of four steel-to-timber connections for possible application to LVL spatial trusses. As the behaviour of slender timber struts may virtually be ruled by buckling, the structural efficiency of connections should initially be verified in tension. Therefore, monotonic pull-pull load tests were carried out, and the relevant results are discussed in this paper. Specifically, the stiffnesses and load-carrying capacities of the following types of connection (Fig. 2) were investigated:

- Type A: dowel-nut connection (Fig. 2a) analogous to those tested in [37], but showing connector's nominal yield strength $f_y = 355$ MPa instead of 1080 MPa;
- Type B: two-bolt dowelled connection with outer steel plates (Fig. 2b);
- Type C: two-bolt dowelled connection with inner steel plate (Fig. 2c);
- Type D: axial threaded insert connection (Fig. 2d).

Given the extremely small cross-section of the tested timber elements, i.e., 50×50 mm, none of the geometric configurations analysed is covered by current design regulations on minimum connectors' edge distances. The experimental assessment of these non-conforming connections is therefore necessary. Also, this study will highlight the advantages and limitations of each type of connection in terms of ease of assembly and aesthetic impact.

3 Proposed connections for LVL spatial truss structures

A schematic representation of a timber spatial truss structure is shown in Fig. 3. The nodes are formed by steel spheres specially shaped and provided with threaded holes according to the directions of the various elements. As a matter of fact, a longitudinal

Fig. 3 Schematic representation of a timber structure with spheres and steel joints

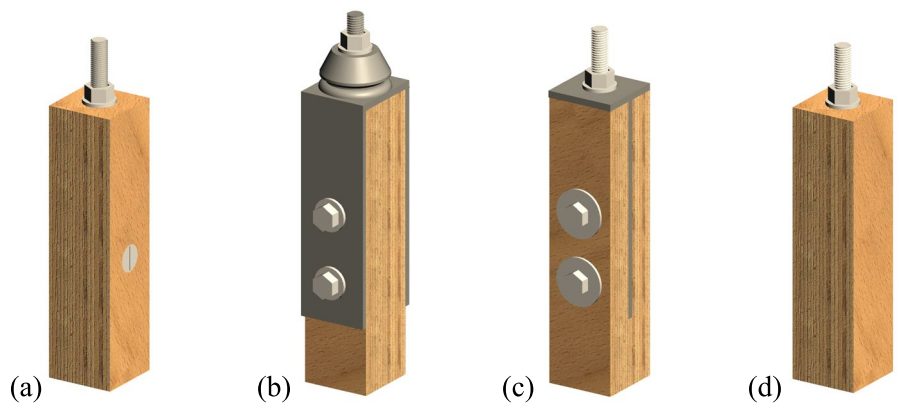

Fig. 2 Investigated connections: **a** type A; **b** type B; **c** type C; and **d** type D

threaded rod (or bolt) will be used at each element end. To allow each member to be easily assembled, this rod must be given sufficient mobility in the axial element direction before screwing into the nodal sphere. Finally, these screwing operations require a suited nut system. In [11], two possible simple technological solutions are described. One of them uses an unthreaded sleeve, made integral with the axial rod due to the presence of a transverse pin (see Sect. 3.2.1 in [11]). The other screwing method is simply based on a double-nut system, which also avoids rod weakening being pin insertion no longer required (see Sect. 3.2.2 in [11]). These two solutions may be equally adopted for all of the proposed connections. That said, this research is focused on tests on individual LVL elements with their end rods connected to the reaction frame, so that none of the described screwing options was needed. A simple hexagonal sleeve or nut has then been screwed onto each threaded rod to avoid specimen misalignments before tests.

The four connection types investigated are described in the following.

3.1 Dowel-nut connection (type A)

This type of connection (Fig. 4) is comprised of a cylindrical steel connector placed transversely to the centroidal axis of the timber element. This connector has a threaded hole, orthogonal to its axis, suited for the longitudinal threaded rod. Therefore, the tensile load transfers from longitudinal rod to timber by means of dowel-nut.

The assembly stages of each specimen end connection are summarized as follows (Fig. 4a):

- Stage 1: drill longitudinal and transverse holes in timber element;
- Stage 2: insert dowel-nut connector in transverse hole;
- Stage 3: insert threaded rod in longitudinal hole and screw it into dowel-nut;
- Stage 4: insert washer and screw hex sleeve (or nut) onto threaded rod; insert axial rod into grip of the reaction frame and adjust.

The dowel-nut can be positioned with its axis either parallel or orthogonal to the veneer layers. The specimen shown in Fig. 4b has the connector orthogonal to the veneers.

To add data to the experimental campaign presented in [37], four more tests on this type of connection are presented hereinafter. In these tests, the connector was orthogonal to the veneers for two of the specimens, and parallel to the veneers for the remaining two specimens.

3.2 Dowelled connection with outer steel plates (type B)

This type of connection (Fig. 5), revising connections relatively common in timber construction, is comprised of two outer steel plates and two bolts placed transversely to the axis of the timber element. The steel plates are mutually connected

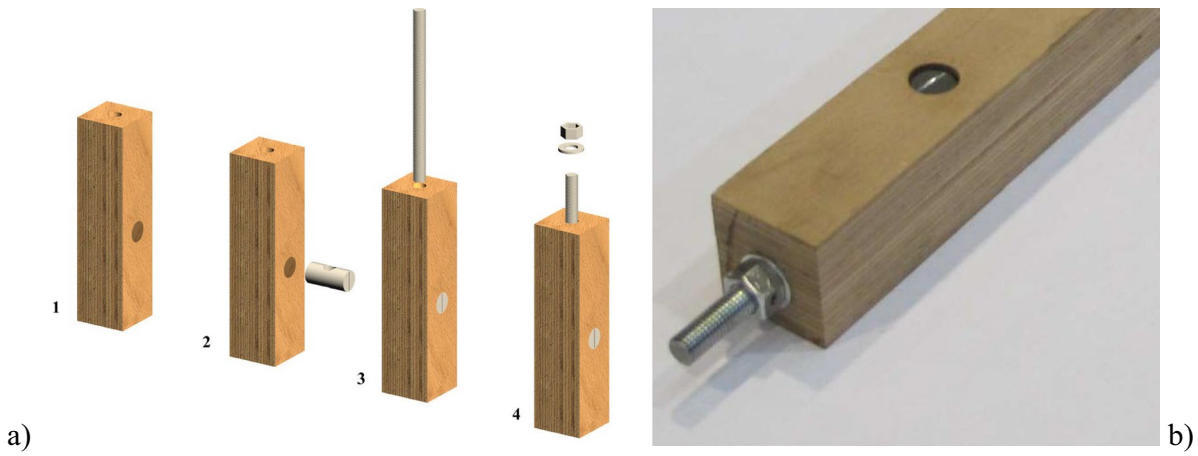

Fig. 4 Type A connection: **a** assembly stages and **b** specimen before test

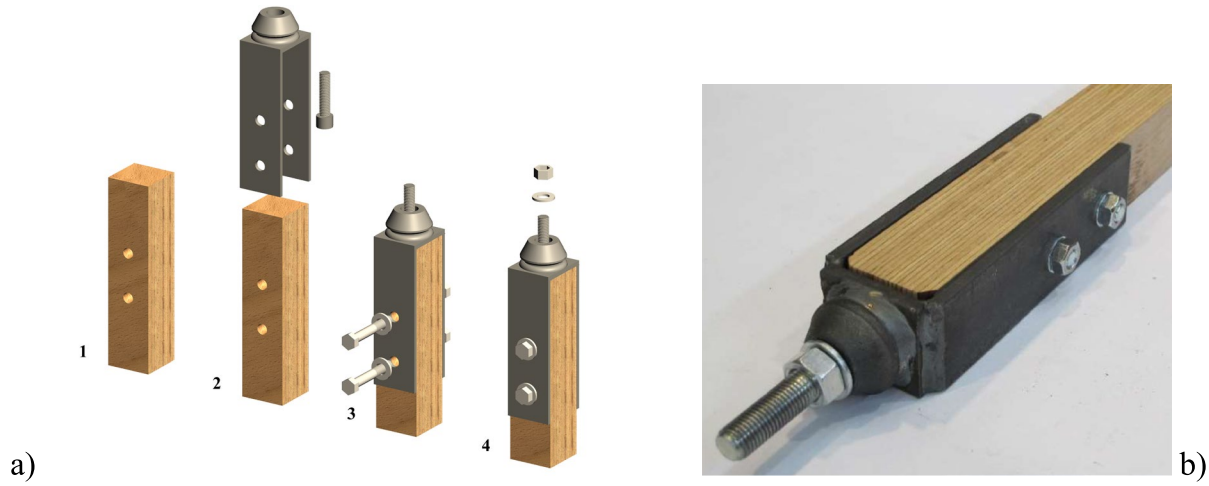

Fig. 5 Type B connection: **a** assembly stages and **b** specimen before test

at the element end section by means of a welded front plate. A highly rigid conical steel sleeve, containing the axial bolt used for connection with the node, is welded to the front plate. The assembly of the timber member within the structure is facilitated by the mobility of the axial bolt inside the conical sleeve. The tensile load is transferred from node to external plates by contact between axial bolt's head and inner surface of the conical sleeve.

The assembly stages of each specimen end connection are summarized as follows (Fig. 5a):

- Stage 1: drill two transverse holes in timber element;
- Stage 2: insert axial bolt into the conical sleeve, and external plates assemblage onto the timber element;
- Stage 3: insert transverse bolts and tighten nuts;
- Stage 4: insert washer and screw hex sleeve (or nut) onto axial bolt; insert axial bolt into grip of the reaction frame and adjust.

For this type of connection, fourteen specimens were tested. The transverse bolts were orthogonal to the veneers for seven of these specimens (see Fig. 5b), and parallel to the veneers for the remaining seven specimens. Moreover, three different end distances were investigated.

3.3 Dowelled connection with inner steel plate (type C)

This connection (Fig. 6), adapting traditional dowelled connections, is comprised of a T-shaped steel plate assemblage and two bolts placed transversely to the axis of the timber element. The plate assemblage includes a front plate and an inner plate welded to one another. The former is provided with a centroidal hole, which accommodates the longitudinal threaded rod used for connection with the node. The inner plate is notched to allow for a sufficient threaded rod's mobility during assembly, as well as for the insertion of a nut.

For each specimen end connection, the assembly stages are as follows (Fig. 6a):

- Stage 1: drill two transverse holes in timber element; notch the element to accommodate the inner plate and drill a superficial axial hole large enough to accommodate the back nut;
- Stage 2: insert threaded rod into front plate of T-shaped plate assemblage; screw threaded rod into back nut;
- Stage 3: insert plate assemblage into element notch; insert transverse bolts and tighten nuts;
- Stage 4: insert washer and screw hex sleeve (or nut) onto axial threaded rod; insert rod into grip of the reaction frame and adjust.

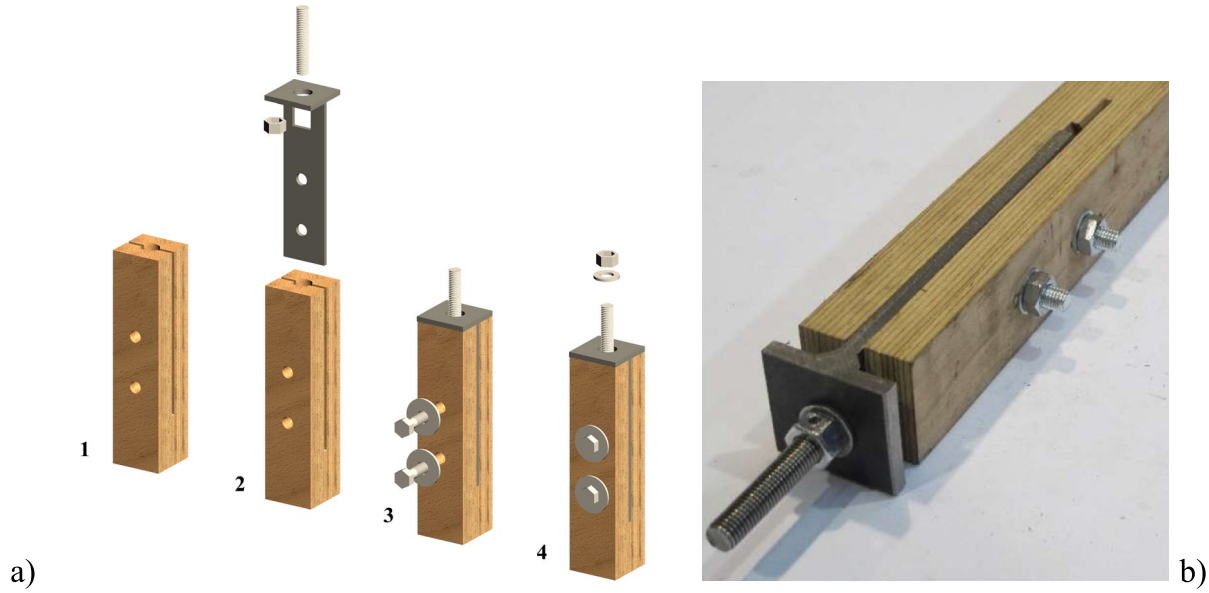

Fig. 6 Type C connection: **a** assembly stages and **b** specimen before test

In the case of axial compression, an efficient load transfer would require the front plate being in contact with timber element end. To this purpose, a further small notch is necessary to accommodate the fillet welds of T-plate assemblage. The compression behaviour of this connection will be investigated through dedicated experiments. Since axial compression is not of concern for this study, the fillet welds were left outside the timber element. This explains the separation between front plate and element end section for the specimen shown in Fig. 6b.

Twelve specimens provided with this type of end connection were tested. The transverse bolts were orthogonal to the veneers for six of these specimens (see Fig. 6b), and parallel to the veneers for the remaining six specimens. In analogy with type B connection, three different end distances were investigated.

3.4 Threaded insert connection (type D)

The last of the connections analysed makes use of a hollow metal screw insert, parallel to the centroidal element axis and provided with internal metric threading. This threading is essential to accommodate the threaded rod required for the end connection with node. Compared to the previous connections, this connection seems extremely fast and practical, as production process is restricted to drilling a pilot hole and, subsequently, screwing of the insert into the timber element. Yet, the extreme care required by these operations must be considered as a potentially strong drawback as even small misalignments between metal insert and timber element may affect structure assembly irretrievably.

The joint mobility is ensured by the depth of the threaded hole in the insert. To allow for the installation of any generic member in a structure, at each element end the threaded rod should initially enter the insert all the way. Then, the rod is gradually unscrewed from the insert to enter the node.

The assembly stages of each specimen end connection may then be summarized as follows (Fig. 7):

- Stage 1: drill pilot hole aligned with specimen centroidal axis;
- Stage 2: screw insert into the timber element;
- Stage 3: screw threaded rod into insert;
- Stage 4: insert washer and screw hex sleeve (or nut) onto axial threaded rod; insert rod into grip of the reaction frame and adjust.

Eight specimens provided with this type of end connection were tested. In all of them, the length of

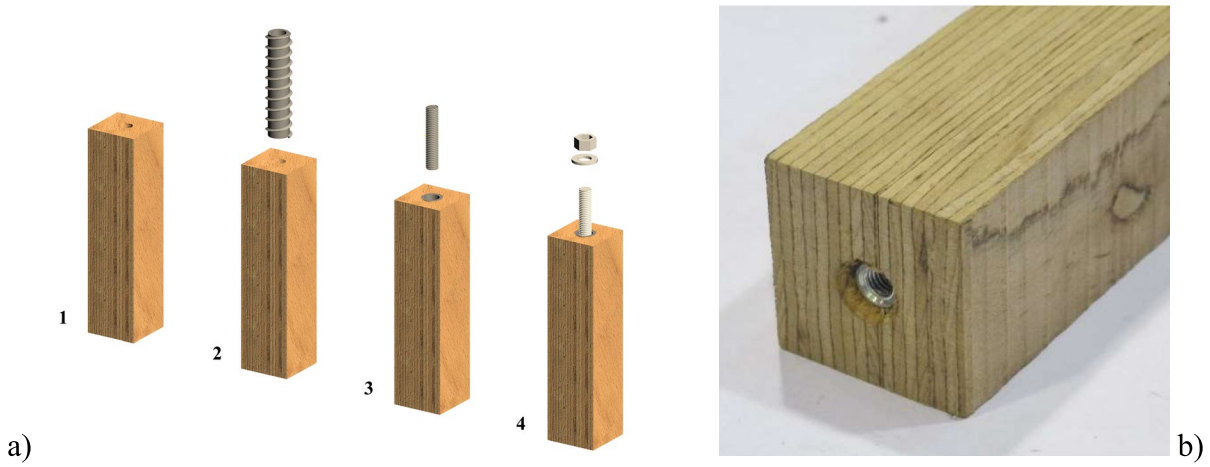

Fig. 7 Type D connection: **a** assembly stages and **b** specimen before screwing of axial threaded rod

the screw insert was of 50 mm. Then, to analyse the effects due to confinement action along the insert depth, four more specimens provided with transverse 6 mm-diameter bolts were tested (see Sect. 3.2). This modified connection will be referred to in the following as type DC connection (=type D Confined).

4 Materials, speciments and methods used in the experiments

The experimental study was conducted at the Civil Engineering Laboratory of the University of Ferrara, using full-scale specimens with the four connection types presented in the previous section.

Described below are mechanical properties of materials, geometric characteristics of specimens, test setup and loading protocol.

4.1 Materials

4.1.1 Steels

To investigate timber failure modes, premature collapse of the axial threaded rods and bolts had to be avoided. This would correspond, in actual spatial trusses, to exclude failure occurrence in close proximity to the nodes, with positive returns on repairability. Therefore, class 12.9 steel ($f_{yb}=1080$ MPa, $f_{ub}=1200$ MPa) was used for these steel components. For analogous reasons, 8 mm-thick plates of grade S355 structural steel ($f_{yk}=355$ MPa, $f_{uk}=490$ MPa) were used in connections B and C. Conversely, to investigate the effects due to yielding of transverse connectors, grade S355 steel was used for dowel-nuts in type A connections, whereas class 8.8 transverse bolts ($f_{yb}=640$ MPa, $f_{ub}=800$ MPa) were adopted in connections B and C.

As accompanying document for the threaded insert used in connections D and DC, the relevant ETA [39] reports manufacturer's designation, intended use, geometric and mechanical properties of various classes of connectors. In the experiments described in this paper, insert BL No. 004 850 6 featuring outer and inner thread diameters of 16 mm and 8 mm, respectively, and overall length of 50 mm was used. Pilot hole diameter was of 12.5 mm as recommended in [39]. Transverse bolts used in connection DC for confinement were of class 12.9 steel. These bolts were applied a tightening torque of 10 Nm, corresponding to about 45% of characteristic ultimate tensile load for a friction coefficient $k=0.15$.

The steel grades for the various metal components used in the experiments are summarized in Table 1.

4.1.2 Beech LVL

The LVL elements used in the experiments belonged to the same batch as specimens described in [37]. They were comprised of 3 mm-thick veneers of regional

Table 1 Steel grades adopted in the tested connections

Connection type	Connection component	Outer diameter or thickness (mm)	Steel class/grade	Reference standard
A	Axial threaded rod	12	12.9	[40]
	Dowel-nut	20	S355	[41]
B	Axial bolt	12	12.9	[40]
	Steel plates	8	S355	[41]
	Transverse bolts	10	8.8	[40]
C	Axial threaded rod	12	12.9	[40]
	Steel plates	8	S355	[41]
	Transverse bolts	10	8.8	[40]
D	Axial threaded rod	8	12.9	[40]
	Threaded insert	16	N.A.(1)	[39]
DC	Axial threaded rod	8	12.9	[40]
	Threaded insert	16	N.A	[39]
	Confining bolts	6	12.9	[40]

(1)N.A. = Not Available, for characteristic resistances in axial tension and bending see [39]

beech wood with grain direction parallel to the longitudinal axis of the specimen and no cross layer. For these products, the highly controlled manufacturing process allows for an even distribution of defects, so ensuring sufficiently homogeneous material properties.

The reader is referred to values of material properties reported in Table 1 of [37], providing a comparison between manufacturer's data derived from the relevant ETA [42] and measured data obtained from specific tests. It is only the case to mention here that mean flatwise bending strength of LVL elements resulted $f_m = 112$ MPa. Moreover, mean and minimum characteristic values of mass density were of 843 kg/m^3 and 680 kg/m^3, respectively. Finally, the moisture content for the specimens tested in this research, estimated by the electrical resistance method [43], was found to lie in the range 8% ± 2%, in line with the climatic conditions recommended for indoor use (see [42]).

5 Summary of experimental tests

A total number of 42 pull-pull tests were carried out (Table 2). The construction details of the various connection are shown in Fig. 8. The designation label for specimens with type A to C connections takes the following form:

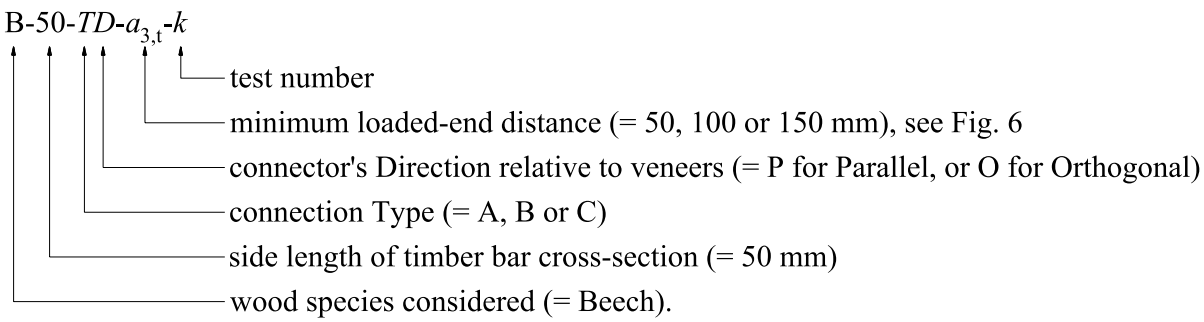

Table 2 Matrix of experimental tests

Test #	Specimen ID	Connection type	Connector direction	Peak capacity (kN)	Displacement at F_{peak} (mm)	Ultimate displacement (mm)	Initial stiffness (kN/mm)
	Symbols			F_{peak}	δ_{peak}	δ_u	K
1	B-50-AO-100-1	A	O	57.7	3.47	3.50	37
2	B-50-AO-100-2	A	O	52.4	2.83	2.83	41
3	B-50-AP-100-1	A	P	47.8	1.79	1.85	36
4	B-50-AP-100-2	A	P	49.6	2.40	2.40	34
5	B-50-BO-50-1	B	O	53.5	2.82	2.91	36
6	B-50-BO-50-2	B	O	60.6	2.71	2.72	36
7	B-50-BP-50-1	B	P	46.8	1.70	1.73	28
8	B-50-BP-50-2	B	P	56.9	2.44	2.44	37
9	B-50-BO-100-1	B	O	71.9	4.98	7.40	22
10	B-50-BO-100-2	B	O	68.9	3.48	4.73	32
11	B-50-BO-100-3	B	O	80.8	5.14	5.35	32
12	B-50-BP-100-1	B	P	81.6	5.19	5.31	24
13	B-50-BP-100-2	B	P	76.2	2.77	2.82	40
14	B-50-BP-100-3	B	P	59.6	2.50	2.53	38
15	B-50-BO-150-1	B	O	71.4	3.76	4.02	37
16	B-50-BO-150-2	B	O	90.1	4.52	4.52	39
17	B-50-BP-150-1	B	P	62.2	2.34	3.52	35
18	B-50-BP-150-2	B	P	72.6	3.00	4.33	41
19	B-50-CO-50-1	C	O	30.5	2.00	2.81	18
20	B-50-CO-50-2	C	O	27.9	1.83	2.00	21
21	B-50-CP-50-1	C	P	34.4	1.14	1.31	57
22	B-50-CP-50-2	C	P	30.8	0.86	0.95	61
23	B-50-CO-100-1	C	O	65.9	4.96	5.88	43
24	B-50-CO-100-2	C	O	59.6	4.01	4.23	18
25	B-50-CP-100-1	C	P	48.9	3.57	3.68	19
26	B-50-CP-100-2	C	P	59.8	4.63	4.64	19
27	B-50-CO-150-1	C	O	65.7	6.14	7.28	31
28	B-50-CO-150-2	C	O	63.4	4.81	8.07	25
29	B-50-CP-150-1	C	P	52.0	3.28	4.92	31
30	B-50-CP-150-2	C	P	46.8	2.30	3.21	40
31	B-50-D16-50-1	D	–	18.3	0.67	–	77
32	B-50-D16-50-2	D	–	17.4	0.57	–	91
33	B-50-D16-50-3	D	–	20.1	0.70	–	74
34	B-50-D16-50-4	D	–	19.3	0.47	–	84
35	B-50-D16-50-5	D	–	18.2	0.42	–	80
36	B-50-D16-50-6	D	–	17.7	0.36	–	66
37	B-50-D16-50-7	D	–	21.3	0.40	–	68
38	B-50-D16-50-8	D	–	18.6	0.38	–	62
39	B-50-DC16-50-1	DC	–	24.8	0.43	–	76
40	B-50-DC16-50-2	DC	–	24.8	0.47	–	66
41	B-50-DC16-50-3	DC	–	25.7	0.47	–	103
42	B-50-DC16-50-4	DC	–	26.7	0.36	–	111

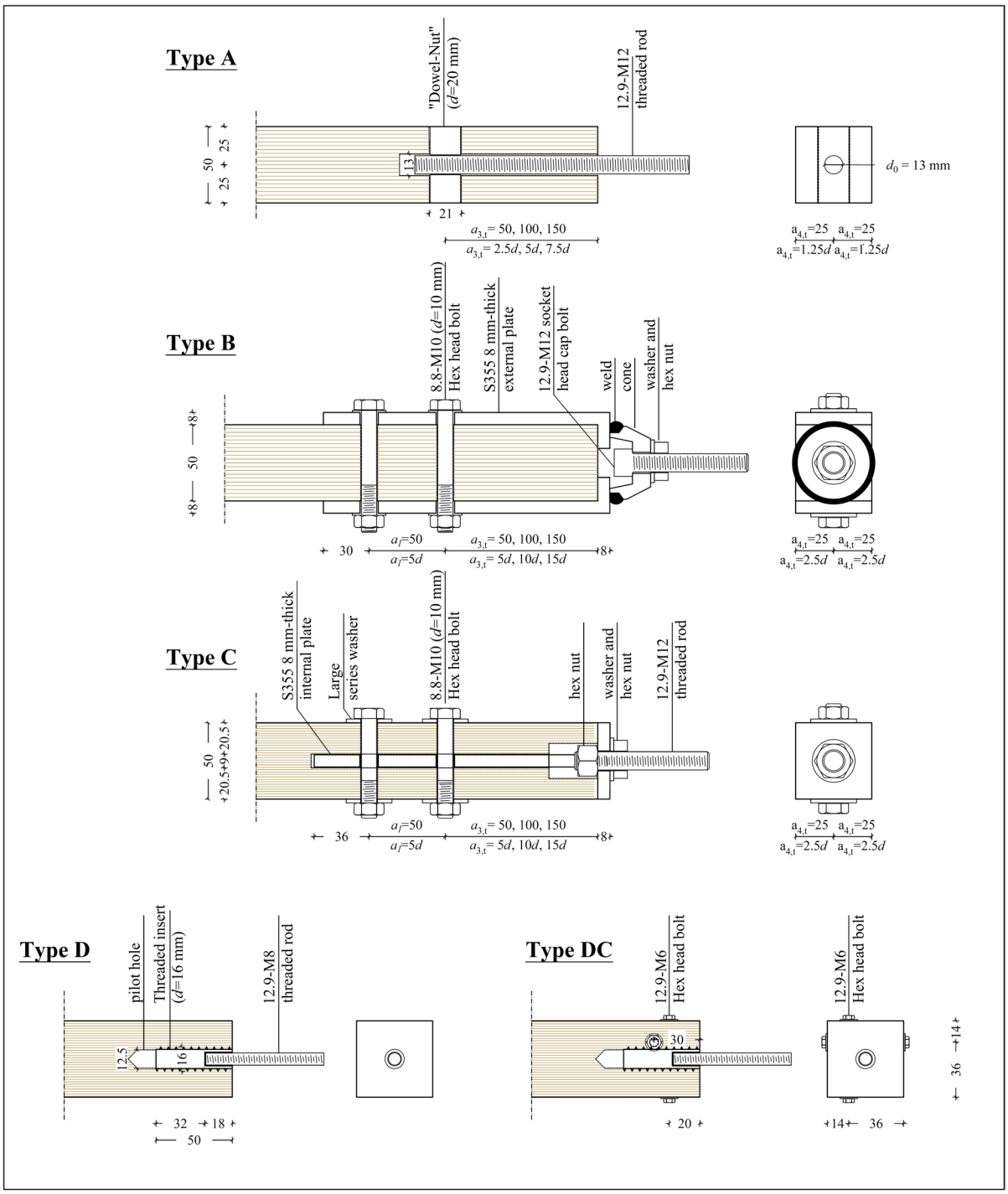

Fig. 8 Construction details of the tested specimens. Dimensions in mm

Note that orientation of dowel-nut or bolts relative to veneers is explicitly identified in the specimen label.

For connections D and DC, threaded inserts with outer diameter and overall length of 16 mm and 50 mm, respectively, were investigated only. Different

Table 3 Comparison between adopted (index "*a*") and recommended (index "*r*") end and edge distances for connections A, B and C. Values in bold font highlight non-conforming configurations

Connection	Loaded-end distance		Edge distance	
	$a_{3,t,a}/d$	$a_{3,t,a}/a_{3,t,r}$	$a_{4,a}/d$	$a_{4,a}/a_{4,r}$
A-50[(1)]	2.5	**0.357**	1.25	**0.417**
A-100	5.0	**0.714**	1.25	**0.417**
A-150[(1)]	7.5	1.071	1.25	**0.417**
B(C)-50	5.0	**0.625**	2.50	**0.833**
B(C)-100	10.0	1.250	2.50	**0.833**
B(C)-150	15.0	1.875	2.50	**0.833**

[(1)]Investigated in [37], relevant experimental results only reproposed in the following for comparison

insert dimensions will be investigated in future studies together with different LVL element cross-sections. Therefore, the designation labels for these connections take account of insert dimensions as follows:

$$\mathrm{B-50-D16-50-}k;\ \mathrm{B-50-DC16-50-}k,$$

where k still specifies the test number.

Symbol $a_{3,t}$ introduced above has the same meaning as in [13]. For bolted connections, setting $a_{3,t}=\max(7d;\ 80\ \mathrm{mm})$ is recommended, with d being fasteners diameter. Moreover, according to the same standard, minimum edge distance of bolts should be $a_{4,t}=a_{4,c}=a_4=3d$. Ratios of adopted to recommended values for both end and edge distances are reported in Table 3 for connection A (see labels of the form A-$a_{3,t}$) and connections B and C (labels B(C)-$a_{3,t}$). Connections A-100 and B(C)-50, as well as connections A-50 tested in [37], presented non-conforming $a_{3,t}$ values. Distances a_4 were non-conforming for all of the type A to C connections.

Although threaded inserts as those adopted in connections D and DC are not strictly covered by standards, they could be considered as axially loaded screws. A minimum angle of 30° between axially loaded screws and grain direction is recommended in [13]. Moreover, the edge distance of screws should be greater than $4d$, with $d=16$ mm indicating (outer) screw diameter. Therefore, none of connections D and DC resulted code-conforming.

In [37], initial tightening torque applied to axial threaded rod was proved to have a strong influence on elastic stiffness of dowel-nut connections. In [38], these preload effects were shown for different connector's end distances, observing that the increase in stiffness with tightening depends on changes in the contact surface between dowel-nut and timber.

As far as type B to D connections are concerned, different axial preload transfer mechanisms are expected. The assessment of preload effects for these connections would require specific round-robin experiments which fall out of the scope of this paper. Therefore, to avoid inconsistencies among the tested specimens, no axial preload was applied in this study. Similarly, in type B and C connections, to exclude any contribution due to friction between steel plates and timber, no transverse preload was applied letting the 10 mm-diameter bolts untightened.

5.1 Test setup and loading protocol

A schematic of the adopted test setup is illustrated in Fig. 9. The tensile load was applied by an electromechanical actuator with loading capacity of 500 kN, stroke length of 500 mm and maximum speed of

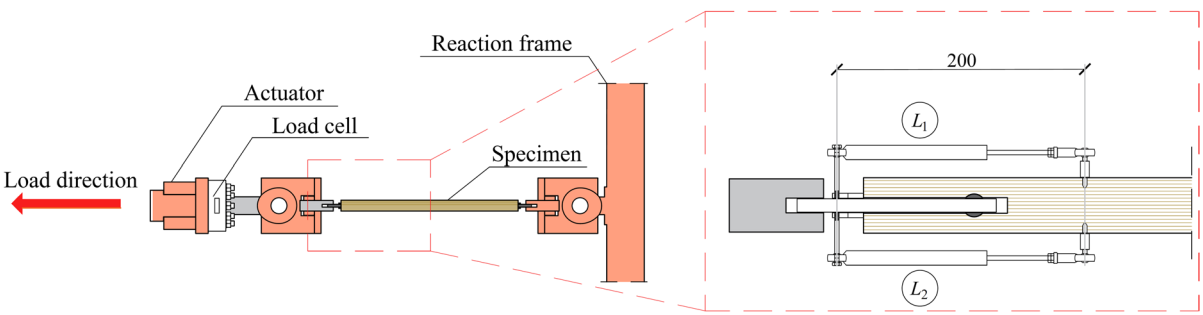

Fig. 9 Experimental setup with zoomed view on linear displacement transducers placed at the specimen end. Dimensions in mm

0.7 mm/s. For load readings (F in the following), a load cell with a nominal sensitivity of 2 mV/V was used. For displacement measurements, a couple of linear displacement transducers with a stroke length of 100 mm was used at each specimen end as shown in Fig. 9. In the force–displacement (F-δ) plots presented hereinafter, displacement δ represents the mean of the two transducers' measurements. Signal acquisition was performed using National Instruments boards and a specifically developed LabVIEW code.

The loading protocol outlined in [44] was adopted. This protocol includes an elastic preloading at approximately $0.4F_{peak,e}$, with $F_{peak,e}$ being the estimated load-carrying capacity, followed by unloading up to $0.1F_{peak,e}$ and then subsequent reloading up to failure. Estimates $F_{peak,e}$ were obtained from preliminary tests. The testing speed was kept constantly equal to approximately $0.2F_{peak,e}$ per minute. Controlling plunger's speed allowed capturing descending branches in the F-δ responses.

6 Experimental results

This section illustrates the results of the experimental tests for each connection type. Reported in Table 2 are load-carrying capacity (F_{peak}), displacement at F_{peak} (δ_{peak}), ultimate displacement (δ_u), and initial stiffness (K) for each of the specimens. Displacement δ_u is provided only for type A to C connections, because residual tensile resistance for connections D and DC resulted non negligible even at very large, impractical displacements (see Sect. 4.4). Initial stiffness is obtained as the slope of a straight line fitted to F-δ data in the range $(0.1 \div 0.4)F_{peak}$.

6.1 Type A connection

In monotonic tests described in [37], dowel-nuts of class 12.9 steel ($f_{yk} = 1080$ MPa) were used to activate wood-side failure in the absence of interaction with yielding of connectors. The F-δ responses obtained in that study are reproposed in Fig. 10a, b and c for $a_{3,t} = 50$ mm, 100 mm, and 150 mm, respectively. Grey and light blue hatched surfaces are related to variability of test results for dowel-nut axis aligned with and orthogonal to, respectively, the veneer planes.

In this study, grade S355 dowel-nuts, showing yield strength reduced by two-thirds, were adopted with $a_{3,t} = 100$ mm. The corresponding F-δ plots are reported in Fig. 10b, where black and blue lines refer to parallel- and orthogonal-to-veneers connectors, respectively. These specimens exhibited elastic behaviour up to $80\% \div 90\%$ of F_{peak}, followed by a progressive stiffness reduction due to yielding of connector, which contributed to a moderate ductility. The mean elastic stiffness resulted $K = 37$ kN/mm. Capacity F_{peak} lying between 47.2 and 56.7 kN, and displacement δ_u of 1.8–3.5 mm were shown (Table 2). The mean of F_{peak} for orthogonal dowel-nut was approximately 13% larger than that for parallel connector. Furthermore, connector's orientation influenced the ultimate displacement, with the greatest δ_u values observed for orthogonal dowel-nuts.

Compared to class 12.9 connectors used in [37], smaller-yield strength dowel-nuts resulted in reduced mean F_{peak} only for orthogonal alignment (-9.1%), as for parallel alignment only a minor influence on capacity was observed (-0.8%). The absence of any preload led, in this study, to strong stiffness reductions.

Timber failure modes were invariably brittle, involving splitting (Fig. 11a), plug shear (Fig. 11b), or a combination of the two (Fig. 11c). Plastic deformation of connectors was observed (Fig. 11d).

6.2 Type B connection

For this connection, 4 tests for end distance $a_{3,t} = 50$ mm, 6 tests for $a_{3,t} = 100$ mm, and 4 tests again for $a_{3,t} = 150$ mm were conducted. The corresponding F-δ plots are shown in Fig. 10d, e, and f, respectively, where colour lines have the same meaning as in Fig. 10b. All specimens exhibited an initial low-stiffness phase. This behaviour occurred at small tensile forces (a few kN) due to transverse bolt-hole clearances. Different extents observed in the figures for this initial phase may have been due to assembly tolerances and/or small tightening unintentionally applied to transverse bolts. Beyond this phase, elastic stiffness resulted relatively little scattered among the 14 tests. Mean and Coefficient of Variation (CoV) of K of 34 kN/mm and 17%, respectively, were obtained (Table 2).

For $a_{3,t} = 50$ mm, elastic behaviour was observed until the development of a plug shear, interlaminar

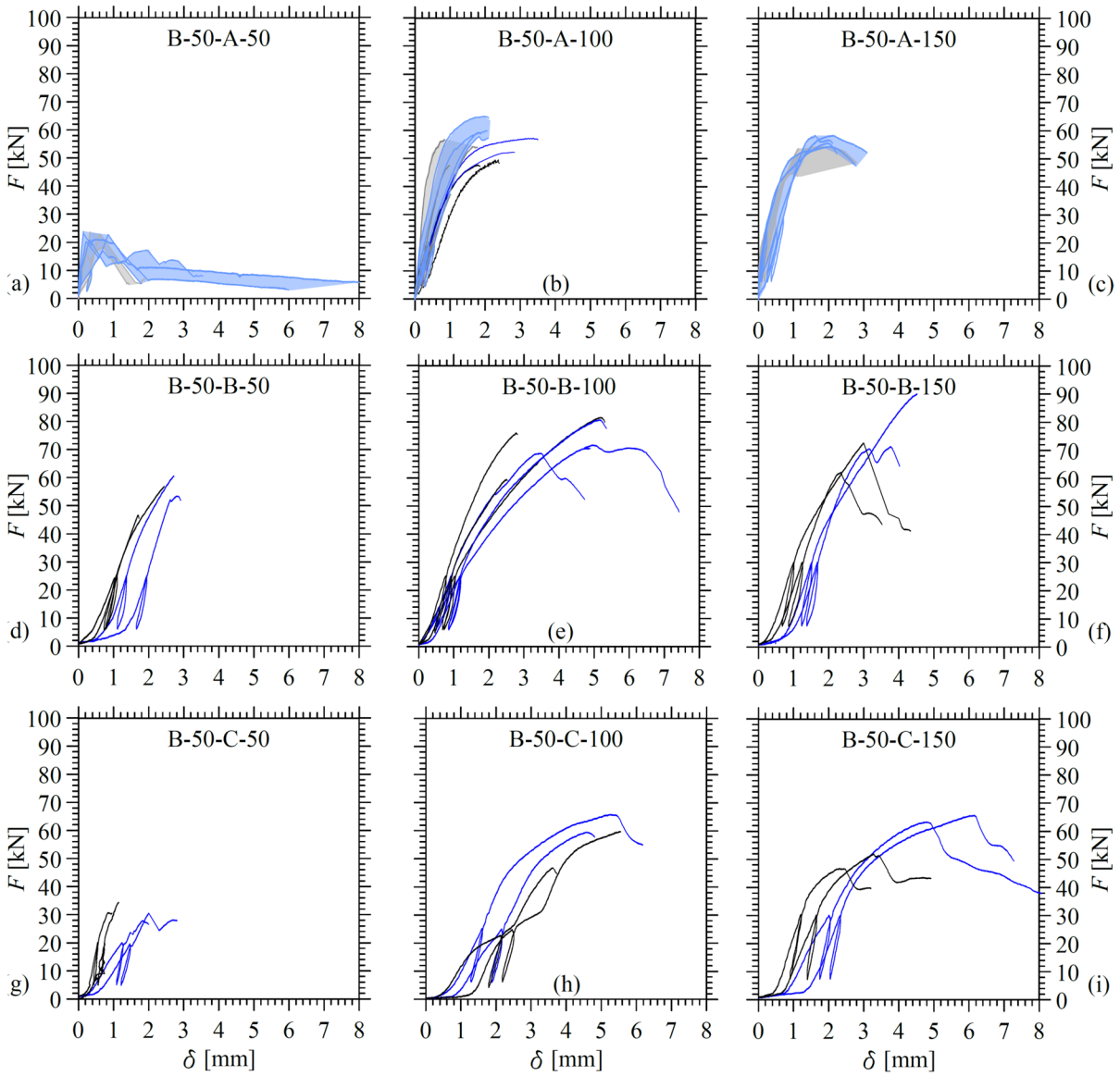

Fig. 10 *F*-δ responses from monotonic pull-pull tests on type **a**, **b**, **c** A; **d**, **e**, **f** B, and **g**, **h**, **i** C connections. Loaded-end distance ($a_{3,t}$): **a**, **d**, **g** 50 mm; **b**, **e**, **h** 100 mm; **c**, **f**, **i** 150 mm. Black and blue lines are for connectors parallel and orthogonal to veneers, respectively. Similarly, gray and light blue hatching in (**a**, **b**, **c**) refer to test results reported in [37] for parallel and orthogonal dowel-nuts, respectively

failure in the front of the first bolt (Fig. 12a). At this stage, a simultaneous timber fracture occurred between the bolts, resulting in an overall brittle failure. Mean load-carrying capacity for transverse bolts orthogonal to veneers was 10.2% greater than that for parallel bolts.

For $a_{3,t}=100$ mm, a significant increase in load-carrying capacity was observed. Specimens with parallel bolt alignment showed elastic-brittle behaviour, with plug shear failure similar to that observed for $a_{3,t}=50$ mm. For specimens with orthogonal bolt alignment, no significant change in mean F_{peak} was obtained and timber failure mode remained brittle (Fig. 12b). However, two of these specimens showed a post-peak load path, resulting in a sort of pseudo-ductile response.

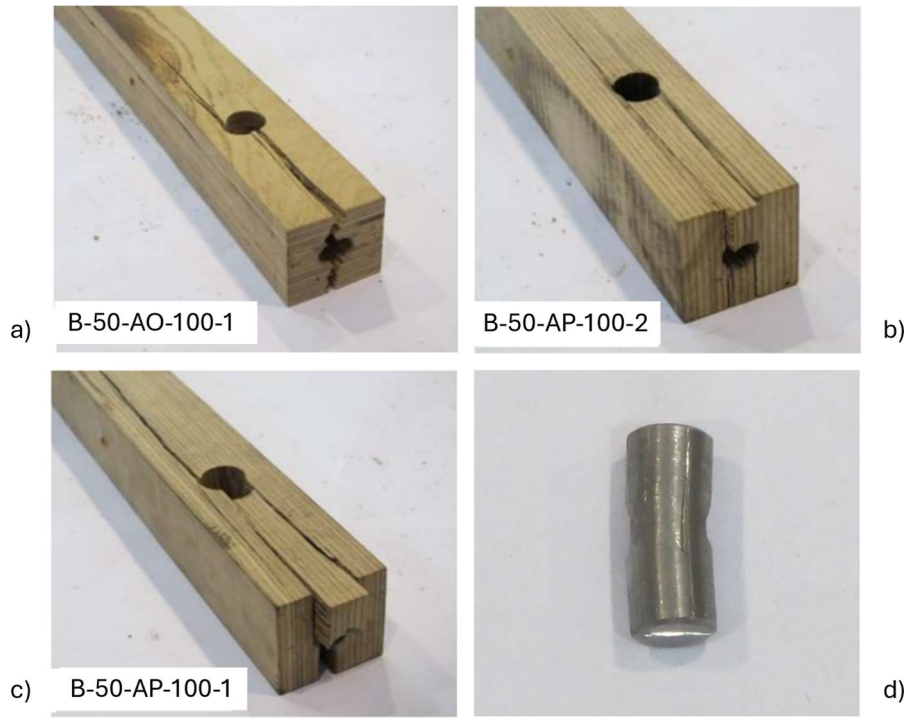

Fig. 11 Observed failure modes for type A connection

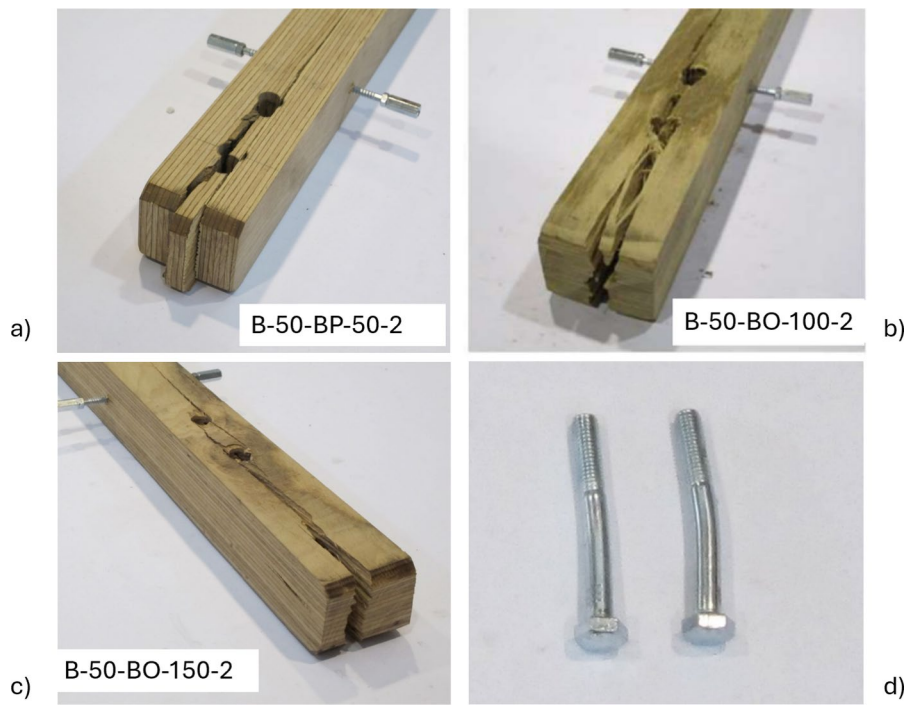

Fig. 12 Observed failure modes for type B connection

For $a_{3,t}=150$ mm, no noticeable, general improvement was observed. Specimen B-50-BO-150-2 exhibited a load-carrying capacity increased by more than 30% compared to mean of F_{peak} for the other specimens (one with orthogonal- and two with parallel-to-veneers bolts). To consider this overstrength as a possible outlier further tests are needed, which will be carried out in a subsequent research stage. In the case of parallel bolts, post-peak paths, but characterized by abrupt resistance drop, were obtained. Brittle (splitting) failure was achieved in all of the tests (Fig. 12c). Therefore, plastic deformation of transverse bolts, observed at the end of test for both $a_{3,t}=100$ mm and 150 mm (Fig. 12d), were not sufficient to yield ductile failure of timber element.

6.3 Type C connection

The F-δ plots for type C connection are shown in Fig. 10g, h and i for $a_{3,t}=50$ mm, 100 mm and 150 mm, respectively. In analogy to the previous connection type, initial low-stiffness responses, characterized by different extents among the various specimens, were observed due to assembly tolerances. This produced an initial slip, particularly evident for some specimens of B-50-C-100 (Fig. 10h) and B-50-C-150 (Fig. 10i) series. The subsequent elastic responses showed extremely scattered stiffnesses, with mean and CoV of 32 kN/mm and 48%, respectively (Table 2). It is then confirmed that the service behaviour of spatial structures using connections of type B and C may be impaired by tolerances and bolt-hole clearance.

For $a_{3,t}=50$ mm, elastic behaviour was observed up to the activation of a plug shear failure in the front of the first bolt. Only test B-50-CO-50-1 exhibited a partial strength recovery after the resistance drop following the achievement of F_{peak}. In this case, the connection failed in plug shear between the two connectors. All of the other specimens failed in plug shear. Specimens with parallel-to-veneers bolts showed mean F_{peak} 12% greater than specimens with orthogonal bolt alignment. The former also resulted very stiffer, probably due to friction caused by unintentional tightening of transverse bolts.

For $a_{3,t}=100$ mm, F_{peak} ranged between 48.9 and 65.9 kN, with δ_u lying in the range $3.7 \div 5.9$ mm. Except for specimen B-50-CO-100-1, which displayed a post-peak degradation, all other specimens failed immediately after the attainment of F_{peak}.

Fig. 13 Observed failure modes for type C connection

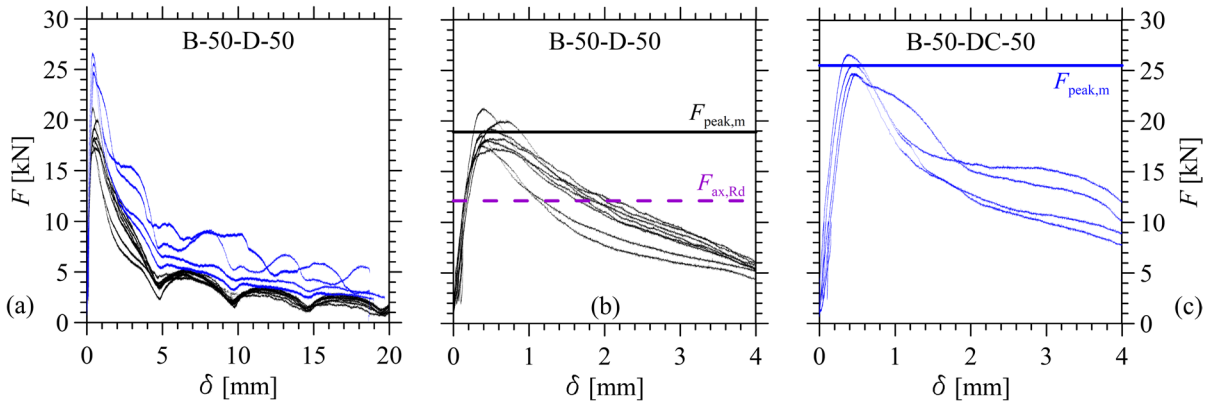

Fig. 14 F-δ responses from monotonic pull-pull tests on **a** type D (black lines) and DC connections (blue lines) for δ ≤ 20 mm, and on type **b** D and **c** DC connections considered separately for δ ≤ 4 mm. Horizontal solid lines in (**b**) and (**c**) are for mean F_{peak}; dashed line in (**b**) is for design withdrawal capacity $F_{ax,Rd}$ (see Sect. 5.2)

Failure modes included plug shear, splitting, or mixed modes (Fig. 13a–c), with no apparent relation with the orientation of transverse bolts. The evident stiffness drops shown between 18 and 32 kN by specimens with parallel bolts, and partly by specimen B-50-CO-100-2, affecting the computed K values, were probably due to release of unintentional friction. For load-carrying capacity exceeding 50 kN, a stiffness reduction was observed due to yielding of transverse bolts (Fig. 13d).

For $a_{3,t} = 150$ mm, mean and CoV of K resulted of 32 kN/m and only 6%, respectively, indicating a very low scatter. Compared to the other $a_{3,t}$ values, a larger deformability was observed in this case in the post-peak region. Plastic deformation of transverse bolts was also evident, but the failure modes remained brittle (Fig. 13c). Connections with orthogonal bolts showed a mean F_{peak} approximately 30% greater than those with parallel bolts.

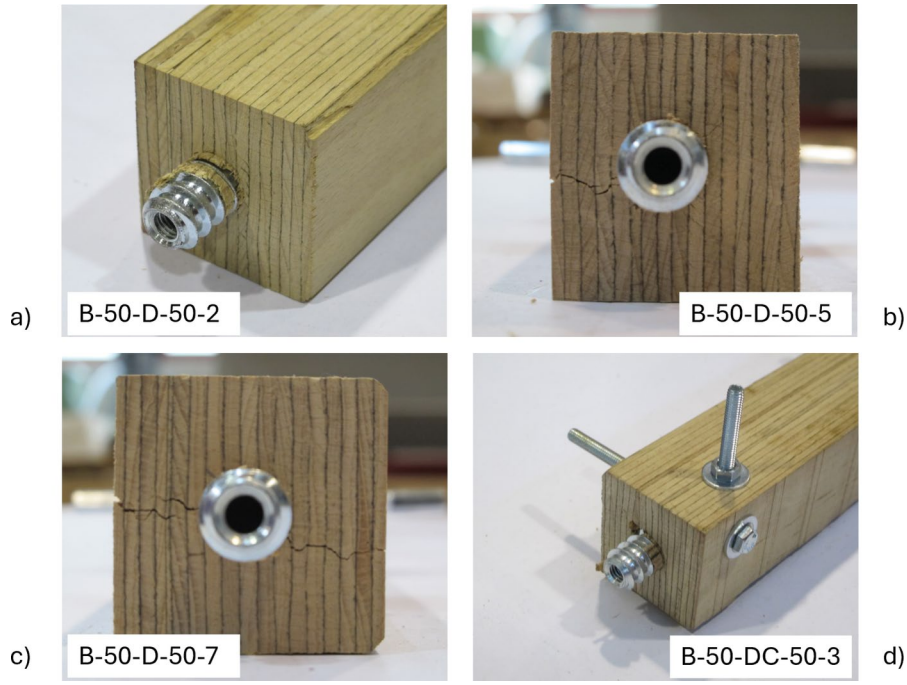

Fig. 15 Observed failure modes for type **a**, **b**, **c** D and **d** DC connections

6.4 Type D and DC connections

The F-δ responses obtained for these connections are reported in Fig. 14a, showing very stiff elastic load paths up to the peak resistance, first followed by an abrupt strength decay and then by a slowly-degrading branch. Detailed representations of the same curves in the displacement range $\delta \leq 4$ mm are reproposed in Fig. 14b for type D connection, and in Fig. 14c for type DC connection only.

As far as type D connection is concerned, the specimens exhibited elastic stiffness ranging between 62 and 91 kN/mm, with mean and CoV of K of 75 kN/mm and 13%, respectively. The load-carrying capacity ranged from 17.4 to 21.3 kN, with a rather limited CoV (7%). Displacement δ_{peak} ranged between 0.36 and 0.70 mm, resulting less scattered compared to the previous connections. The failure mode was always characterized by insert pullout (Fig. 15a). For 7 out of 8 specimens, pullout was accompanied by splitting cracks developing, either parallel or orthogonal to veneers, across a half (Fig. 15b) or the entirety of the cross-section depth (Fig. 15c). After the achievement of F_{peak} and pullout initiation, δ measurements substantially coincided with relative displacements between metal insert and timber element. The residual load-carrying capacity was approximately 25% of F_{peak} for slip $\delta = 5$ mm, coinciding with the thread pitch of the insert. The subsequent series of weak strength recoveries interrupted by further decays exactly recurred at every 5 mm.

In type DC connection, the use of confining bolts resulted in a 17% increase in mean K. Moreover, a 35% increase in mean F_{peak} and a simultaneous halving of CoV of resistance values were observed.

For two of the specimens, a pure pullout mode with no crack formation was shown (Fig. 15d).

7 Comparisons and discussion

Load-carrying capacity predictions based on available design equations are provided in this section. Current design methods (see [13]) were originally formulated for softwood solid timber and glulam, and recommend minimum end and edge distances which have not (or not always) been met in specimens investigated in this study (see Table 3). Moreover, these methods suppose the development of ductile failure, which never took place in the described tests. Therefore, their application to the present LVL-element end connections has a purely comparative purpose. The discussion reported below also suggests possible research developments.

7.1 Shear capacity of dowelled connections

According to the design method presented in § 8.2.3 of [13], Johansen's model assuming rigid behaviour of transverse connectors, with no plastic hinge formation, turns out to be the governing formulation for type A to C connections. As a matter of fact, were

Table 4 Load-carrying capacity from Johansen's model: predictions using embedment strength from Eq. 8.32 reported in [13]

Parameter	Units	Connection type		
		A	B	C
D	[mm]	20	10	10
A_h [(1)]	[mm^2]	$dl - \pi d_0^2/4 = 867$	$dt = 500$	$dt = 410$
n_{ef} [(2)]	[-]	1	$n^{0.9}[a_1/(13d)]^{0.25} = 1.47$	$n^{0.9}[a_1/(13d)]^{0.25} = 1.47$
Capacity predictions from EN 1995 equation for f_h [13]				
Mean capacity				
$f_{h,m} = 0.082(1 - 0.01d)\rho_m$	[MPa]	55.3	62.2	62.2
$F_{Rm} = n_{ef} f_{h,m} A_h$	[kN]	48.0	45.7	37.5
Characteristic and design capacities				
$f_{h,k} = 0.082(1 - 0.01d)\rho_k$	[MPa]	44.6	50.2	50.2
$F_{Rk} = n_{ef} f_{h,k} A_h$	[kN]	38.7	36.9	30.2
$F_{Rd} = k_{mod} F_k/\gamma_M$ [(3)]	[kN]	35.5	33.8	27.7

[(1)] For type A connection, $l = 50$ mm and $d_0 = 13$ mm. For type B and C connections, $t = 50$ mm and 41 mm, respectively

[(2)] For type B and C connections, $n = 2$ and $a_1 = 50$ mm

[(3)] $k_{mod} = 1.1$ (see Table 3.1 in [13] for istantaneous action) and $\gamma_M = 1.2$ (see Table 2.3 in [13])

dowels plasticity be accounted for, Johansen's model for fasteners with characteristic yield moment $M_{y,Rk}$, and including the rope effect through term $F_{ax,Rk}/4$ (which, in turn, may take place for type B and C connections only), would provide an increased shear capacity. This can easily be shown using Eqs. (8.9) to (8.13) reported in [13].

Therefore, the characteristic shear capacity for the investigated dowelled connections may be estimated from the following equation:

$$F_{Rk} = n_{ef} f_{h,k} A_h, \quad (1)$$

where $f_{h,k}$ is the characteristic embedment strength, whereas A_h and n_{ef} represent timber area subjected to $f_{h,k}$ and effective number of transverse connectors, respectively. In Table 4, the calculations of F_{Rk} for mass density $\rho_k = 680$ kg/m^3 (see Sect. 3.1.2), and of design shear capacity F_{Rd} are reported. Under the assumption that the expression for mean embedment strength $f_{h,m}$ takes the same form as that for $f_{h,k}$ (see Eq. 8.32 [13]), but with $\rho_m = 843$ kg/m^3 in the place of ρ_k, Table 4 also reports the calculation of mean shear capacity F_{Rm} according to Johansen's model.

To directly compare the experimental capacities (F_{peak}) provided in Table 2 with F_{Rm} predictions, ratios $\alpha_m = F_{peak}/F_{Rm}$ are reported versus nondimensional end distance in Fig. 16a, b and c for type A, B and C connections, respectively. Blue and red solid circles in the figures are for connectors orthogonal (O) and parallel (P) to veneers, respectively. Grey diamond symbols in Fig. 16a correspond to F_{peak} values for dowel-nut connections tested in [37]. White regions in the plots locate non-conforming connections showing end distance not complying with minimum Eurocode 5 requirements (as far as lateral-edge distance is concerned, non-conformity has already been highlighted for all of the tested connections, see Table 3). Horizontal lines for $\alpha_m = 1$ and F_{Rd}/F_{Rm} are also reported in Fig. 16 for comparison.

For $a_{3,t}/d = 5$, the overstrength shown by connections A and B with orthogonal connectors was significant, with mean α_m resulting of 1.15 and 1.25, respectively. For the parallel series, mean overstrength reduces to 1.02 and 1.13, respectively. The observed performance was in line with, or even superior to, that deducted from $f_{h,m}$ given in [34] for the case of no cross-layer and code-conforming lateral-edge distance a_4. At equal end distance, mean α_m for connection C results of 0.78 for orthogonal bolts and 0.87 for parallel bolts.

For larger $a_{3,t}$, the code predictions systematically underestimate the experimental results, with α_m values ranging between 1.25 (type C, $a_{3,t}/d = 15$) and 1.79 (type B, $a_{3,t}/d = 10$) for parallel series, and between 1.51 (type B, $a_{3,t}/d = 10$) and 1.97 (type B, $a_{3,t}/d = 15$) for orthogonal series.

These results indicate that in high-density wood products brittle connection failure may occur for remarkably high resisted loads. The superior performance of these materials also suggests the need for

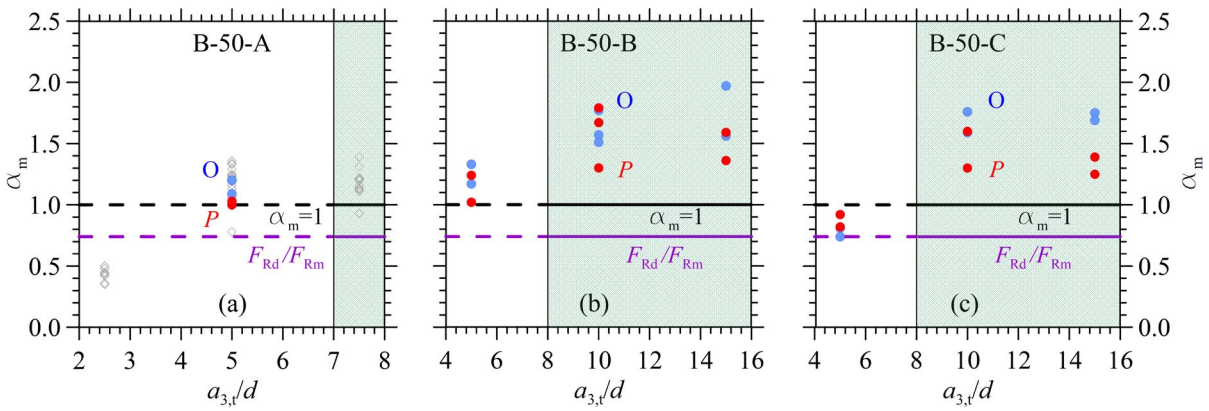

Fig. 16 Ratios $\alpha_m = F_{peak}/F_{Rm}$ of experimental to predicted mean load-carrying capacity versus $a_{3,t}/d$ for type **a** A, **b** B, and **c** C connections. Blue and red circles identify Orthogonal (O) and Parallel (P) fastener arrangement, respectively. Also reported are ratios $\alpha_m = 1$ and F_{Rd}/F_{Rm} (see Table 4)

further studies addressing the development of specific design methods with modified requirements for minimum end and edge distances.

7.2 Axial withdrawal capacity of screwed connections

According to current version of Eurocode 5, axially loaded screws oriented at an angle $\alpha \geq 30°$ to the grain are only allowed, so that design method presented in § 8.7.2 of [13] cannot be used for type D connection. Accompanying document [39] allows for the use of threaded inserts with $0° \leq \alpha \leq 90°$, but the relevant design equation, probably affected by a calibration for softwood, provides too conservative capacity predictions. As a matter of fact, the characteristic withdrawal parameter perpendicular to grain suggested for LVL is $f_{ax,k} = 13$ MPa independently of thread diameter, which seems excessively on the safe side compared to that reported in [45] for self-tapping screws. For screws of diameter $d = 9$ mm in beech LVL, this last document provides $f_{ax,k} = 35$ MPa for associated density $\rho_a = 730$ kg/m^3 and characteristic density lying in the range 590 kg/m$^3 \leq \rho_k \leq 750$ kg/m^3. Moreover, a minimum edge distance of $3d$ is required. Therefore, screws as the adopted insert with $d = 16$ mm in small beech LVL cross-sections with breadth of 50 mm violate any design rule and still need tailored investigations. Anyway, pending further studies, the formulation proposed in [45] may in principle be adopted, yielding characteristic withdrawal capacity in the grain direction ($\alpha = 0$) in the form:

$$F_{ax,Rk} = 0.5 f_{ax,k} d l_{ef} (\rho_k / \rho_a)^{0.8}, \quad (2)$$

where l_{ef} is the insert length (= 50 mm for the adopted insert). For $\rho_k = 680$ kg/m^3, $F_{ax,Rk} = 13.2$ kN and $F_{ax,Rd} = k_{mod} F_{ax,Rk}/\gamma_M = 12.1$ kN (see dashed line in Fig. 14b).

Black and blue solid horizontal lines in Fig. 14b and c locate experimental mean withdrawal capacity for D and DC series, respectively. Mean withdrawal capacity could be also estimated through equations of the form $F_{ax,Rm} = 0.5\, f_{ax,m}\, d\, l_{ef}$, derived from Eq. (2). Substituting mean F_{peak} for type D connection (= 18.9 kN) into the left-hand side of this equation and solving for the withdrawal parameter would lead to $f_{ax,m} = 47.2$ MPa, a very high value compared to data available in current technical documents. A further, significant improvement was achieved due to transverse confinement, which for type DC connection led to $f_{ax,m} = 63.8$ MPa (+35%).

It is worth noting that f_{ax} in Eq. (2) has the meaning of withdrawal parameter as defined in EN 1382 [46] for specific test providing peak capacity F_{peak}, i.e., $f_{ax} = F_{peak}/(dl_{ef})$. Then, this parameter differs from withdrawal strength defined as $f_{ax} = F_{peak}/(\pi dl_{ef})$. Mean withdrawal strength obtained from tests on type D and DC connections results to be of 7.5 MPa and 10.1 MPa, respectively. For solid beech, in [35] mean withdrawal strength $f_{ax} = 12.8$ MPa was attained in grain direction, and larger values (around 22 MPa) were found in tangential and radial directions. However, smaller diameter screws ($d = 5$ mm) in 50 × 50 mm transverse timber sections were used in [35], so that size effects and very large edge distances ($a_4 \geq 4.5d$) may have played a role. Moreover, a smaller pilot hole diameter was adopted in [35] (about 60% of thread diameter, compared to 80% adopted in this study).

Type D connection seems promising for application to LVL spatial structures, especially due to its superior stiffness compared with dowel-type connections. Expressions of the form of Eq. (2) suggest that withdrawal capacity may be improved by increased insert lengths. However, the development of splitting cracks in small-size sections may lead to premature failure, and must probably be controlled by adequate lateral confinement in the light of what it was shown for type DC connection.

8 Conclusions

Geometrical requirements outlined in current technical standards, introduced to prevent brittle failures, effectively hinder the use of hardwood members with small cross-sections. The growth of hardwood applications across timber construction then raises the need for the experimental characterisation of non-conforming connections.

In this paper, 42 pull-pull tests on four types of steel-to-timber connections in beech LVL specimens, including three dowel-type connections and one screwed connection, were presented. The experiments were not aimed at a simple comparison of mechanical performance. The main research objective was rather an exploratory study for potential applications

of these connections to spatial structures featuring high-performance timber elements with reduced cross-sections. Connectors' positioning within square cross-section member does not comply with Eurocode 5 geometrical limitations. Specifically, non-conforming lateral-edge distances were adopted for all of the specimens. Also one of the investigated loaded-end distances for each of the dowelled connections was non-conforming, as well as connector's inclination angle with respect to the veneer planes for the screwed connection.

The most significant results obtained from tests can be summarized as follows.

- For all of the tested connections, the experimental load-carrying capacity exceeded code-based predictions of design resistance; this was also true, in particular, for dowelled connections featuring non-conforming loaded-end distance.
- Dowelled connection with outer steel plates (type B) showed remarkable load-carrying capacity combined with ease of assembly. The conical sleeve at element end facilitates the integration of timber member into the spatial structure. However, a significant steel usage is required, resulting in greater visual impact and costs compared with dowel-nut (type A) and screwed connections (type D).
- A reduction in material usage and visual impact was achieved using internal plates (see type C connection). However, this came at the expense of a reduction in load-carrying capacity ranging from 15 to 50%, depending on the analyzed geometry. This connection retains simplicity in assembly but requires more extensive machining of the timber member, impacting on costs.
- Fit tolerances between plates, bolts and timber, essentially due to bolt-hole cleareances, may result in significant initial slip affecting the elastic response of dowelled connections. For connection with inner plate (type C), this also reflected on a highly scattered initial stiffness (CoV = 48%). To overcome this drawback, transverse bolts should be preloaded to activate frictional strength between steel plate(s) and timber. Preload magnitude should be tuned based on dedicated experiments.
- The dowel-nut connection, which remains concealed within the timber member, combines limited steel usage, ease of assembly, and high mechanical performance. Increased, little scattered stiffness can be achieved by applying a tightening torque to the axial threaded rod, as shown in [11, 37] and [38].
- The threaded-insert connection (type D) is backlash-free. Thus, it exhibited the highest elastic stiffness. However, this connection requires high installation precision, because even small insert deviations from alignment with longitudinal element axis may complicate the assembly process. While the load-carrying capacity was modest compared to other proposed solutions, it could in theory be improved by increasing the insert length (to be confirmed by future studies).
- Transverse confinement of threaded-insert connection, achieved using bolts perpendicular to the insert's axis (so obtaining type DC connections), resulted in a 35% increase in load-carrying capacity and a 50% reduction of correponding CoV. Moreover, the elastic stiffness increased by 17%.

In view of these findings, future research will include multiple studies focused on the dowel-nut and threaded insert connections in LVL specimens. These studies will investigate various specimen geometries and connectors dimensions, to assess configurations beyond those addressed by current design codes. Additionally, the research will be expanded to include other timber species, such as spruce, which has reduced, but still relevant mechanical performance compared with beech, and could then be exploited more effectively.

High-performance products like LVL may yield remarkable advantages to timber construction, but further investigations are necessary to fully harness their capabilities.

Acknowledgements The present investigation was developed in the framework of the industrial innovation project TIRISICO (PG/2015/737636) granted by Regione Emilia-Romagna, POR-FESR 2014-2020 (Region Operational Program for the European Regional Development Fund). The test specimens were supplied by Bozza srl in Busa di Vigonza, Padua, Italy.

Funding Open access funding provided by Università degli Studi di Ferrara within the CRUI-CARE Agreement.

Data availability All information needed for replicating the experimental tests has hopefully been reported in the text. Raw

data such as displacement and load measurements will be made available on request.

References

1. Sathre R, O'Connor J (2010) A Synthesis of Research on Wood Products & Greenhouse Gas Impacts, 2010, 2nd Edition. Technical Report No. TR-19R, FPInnovations, Vancouver
2. Gustavsson L, Nguyen T, Sathre R, Tettey UYA (2021) Climate effects of forestry and substitution of concrete buildings and fossil energy. Renew Sustain Energy Rev 136:110435. https://doi.org/10.1016/j.rser.2020.110435
3. Bukauskas A, Mayencourt P, Shepherd P, Sharma B, Mueller C, Walker P, Bregulla J (2019) Whole timber construction: a state of the art review. Constr Build Mater 213:748–769. https://doi.org/10.1016/j.conbuildmat.2019.03.043
4. Burton R, Dickson M, Harris R (1998) The use of roundwood thinnings in buildings – a case study. Build Res Inf 26(2):76–93. https://doi.org/10.1080/096132198370001
5. Brito LD, Calil C Jr (2010) Manual of design and construction of structures with round pieces of reforestation wood. Cadernos de Engenharia de Estrutturas, Saõ Carlos 12(56):57–77
6. Xiao Y, Chen G, Feng L (2014) Experimental studies on roof trusses made of glubam. Mater Struct 47:1879–1890. https://doi.org/10.1617/s11527-013-0157-7
7. Hua H, Hovestadt L, Li B (2022) Reconfigurable modular system of prefabricated timber grids. Comput Aided Des 146:03230. https://doi.org/10.1016/j.cad.2022.103230
8. Chilton JC, Tang G (2016) Timber gridshells – architecture, structure and craft, 1st edn. Routledge, London
9. Crocetti R (2016) Large-Span Timber Structures. In: Proceedings of the World Congress on Civil, Structural, and Environmental Engineering (CSEE'16), Prague. https://doi.org/10.11159/icsenm16.124.
10. Kunecký J, Arciszewska-Kędzior A, Sebera V, Hasníková H (2016) Mechanical performance of dovetail joint related to the global stiffness of timber roof structures. Mater Struct 49:2315–2327. https://doi.org/10.1617/s11527-015-0651-1
11. Fabbri A, Minghini F, Tullini N (2025) Timber spatial trusses using laminated veneer lumber. J Build Eng 100:111696. https://doi.org/10.1016/j.jobe.2024.111696
12. Azinović B, Serrano E, Kramar M, Pazlar T (2018) Experimental investigation of the axial strength of glued-in rods in cross laminated timber. Mater Struct 51:143. https://doi.org/10.1617/s11527-018-1268-y
13. European Committee for Standardization, EN 1995-1-1:2004/A2:2014. Eurocode 5: Design of Timber Structures – Part 1–1: General – Common Rules and Rules for Buildings.
14. Johansen K (1949) Theory of timber connections. Int Assoc Bridge Struct Eng Publ 9:249–262
15. Meyer A (1957) Die Tragfähigkeit von Nagleverbindungen bei statischer Belastung. Holz als Roh- und Werkstoff 15(2):96–109
16. Jorissen AJM (1998) Double shear timber connections with dowel type fasteners. Delft University Press, Delft
17. Sandhaas C, Blaß HJ (2017) Timber engineering – principles for design. KIT Scientific Publishing, Karlsruhe. https://doi.org/10.5445/KSP/1000069616
18. Mohammad M, Quenneville JHP (2001) Bolted wood–steel and wood–steel–wood connections: verification of a new design approach. Can J Civ Eng 28(2):254–263. https://doi.org/10.1139/l00-105
19. Sjödin J, Johansson C-J (2007) Influence of initial moisture induced stresses in multiple steel-to-timber dowel joints. Holz als Roh- und Werkstoff 65:71–77. https://doi.org/10.1007/s00107-006-0136-6
20. Sjödin J, Serrano E, Enquist B (2008) An experimental and numerical study of the effect of friction in single dowel joints. Holz als Roh- und Werkstoff 66:363–372. https://doi.org/10.1007/s00107-008-0267-z
21. Quenneville JHP, Mohammad M (2001) Design method for bolted connections loaded perpendicular-to-grain. Can J Civ Eng 28(6):949–959. https://doi.org/10.1139/l01-059
22. Mohammad M (2007) Improved Design Procedure for Timber Bolted Connections. Forintek Canada Corp., Project No. 4914, Canadian Forest Service No. 3, Final Report 2006/07
23. Canadian Standard Association, CSA 086:14 (R2019). Engineering design in wood
24. Morgado TFM, Dias AMPG, Machado JS, Negrão JH (2013) Structural connections for small-diameter poles. J Struct Eng 139(11):2003–2009. https://doi.org/10.1061/(ASCE)ST.1943-541X.0000752
25. Romero A, Odenbreit C (2023) Experimental investigation on strength and stiffness properties of laminated veneer lumber (LVL). Materials 16(22):7194. https://doi.org/10.3390/ma16227194
26. Zhang D, Wang Z, Bilal H, Shen Z, Zhou Y (2024) Study on elastic constants of laminated veneer lumber by dynamic test. Mater Struct 57:98. https://doi.org/10.1617/s11527-024-02364-4
27. Li M, He M, Shen Z (2024) Compressive behavior of Australian radiata pine laminated veneer lumber. Mater Struct 57:182. https://doi.org/10.1617/s11527-024-02458-z
28. Balasbaneh AT, Sher W, Yeoh D, Yasin MN (2023) Economic and environmental life cycle perspectives on two engineered wood products: comparison of LVL and GLT construction materials. Environ Sci

Pollut Res 30:26964–26981. https://doi.org/10.1007/s11356-022-24079-1
29. Bader TK, Schweigler M, Hochreiner G, Enquist B, Dorn M, Serrano E (2016) Experimental characterization of the global and local behavior of multi-dowel LVL-connections under complex loading. Mater Struct 49:2407–2424. https://doi.org/10.1617/s11527-015-0657-8
30. Jensen JL, Quenneville P, Girhammar UA, Källsner B (2012) Splitting of timber beams loaded perpendicular to grain by connections–combined effect of edge and end distance. Constr Build Mater 35:289–293. https://doi.org/10.1016/j.conbuildmat.2012.04.006
31. Nguyen HH, Gilber BP, McGavin RL, Bailleres H, Karampour H (2020) Embedment strength of mixed-species laminated veneer lumbers and cross-banded laminated veneer lumbers. Eur J Wood Wood Prod 78:365–386. https://doi.org/10.1007/s00107-020-01504-1
32. Kobel P, Frangi A, Steiger R (2014) Dowel-type connections in LVL made of beech wood, in: Proceedings of the first International Network on Timber Engineering Research (INTER), Bath, United Kingdom, 2014, pp. 103–115.
33. Kobel P, Steiger R, Frangi A (2014) Experimental analysis on the structural behaviour of connections with LVL made of beech wood. RILEM Bookser 9:211–220. https://doi.org/10.1007/978-94-007-7811-5_20
34. Kobel P (2019) Dowel-type connections in beech LVL. PhD Thesis, Diss. ETH No. 26172, Zürich, Switzerland, 2019. Available at https://www.research-collection.ethz.ch/handle/20.500.11850/407651.
35. Celebi G, Kilic M (2007) Nail and screw withdrawal strength of laminated veneer lumber made up hardwood and softwood layers. Constr Build Mater 21(4):894–900. https://doi.org/10.1016/j.conbuildmat.2005.12.015
36. Taj MA, Kazemi NS, Ebrahimi G (2009) Withdrawal and lateral resistance of wood screw in beech, hornbeam and poplar. Eur J Wood Wood Prod 67:135–140. https://doi.org/10.1007/s00107-008-0294-9
37. Fabbri A, Minghini F, Tullini N (2022) Monotonic and cyclic pull-pull tests on dowel-nut connector in laminated veneer lumber made of European beech wood. Constr Build Mater 359:129461. https://doi.org/10.1016/j.conbuildmat.2022.129461
38. Benvenuti E, Fabbri A, Minghini F, Orlando N, Tullini N (2024) 3D orthotropic damage model for the failure analysis of LVL wood truss with steel connector through a regularized extended finite element method. Finite Elem Anal Des 233:104125. https://doi.org/10.1016/j.finel.2024.104125
39. European Technical Assessment ETA-12/0481 of 2021/03/22. Available at https://www.rampa.com/media/35/3f/9c/1671462200/ETA120481%20HB%20RAMPA%20r3%202020_22_03_2021.pdf
40. European Committee for Standardization, EN ISO 898-1: 2013. Mechanical properties of fasteners made of carbon steel and alloy steel – Part 1: Bolts, screws and studs with specified property classes – Coarse thread and fine pitch thread
41. European Committee for Standardization, EN 1993-1-1:2022. Eurocode 3: Design of Steel Structures – Part 1–1: General rules and rules for buildings.
42. European Technical Assessment ETA-14/0354 of 2015/02/20. Available at https://neueholzbau.ch/wp-content/uploads/sites/3/2018/09/ETA_BauBuche-Beam-GL70_140354_0215-EN.pdf.
43. European Committee for Standardization, EN 13183-2:2002. Moisture Content of a Piece of Sawn Timber. Estimation by Electrical Resistance Method
44. European Committee for Standardization, EN 26891:1991. Timber structures – Joints made with mechanical fasteners – General principles for the determination of strength and deformation characteristics.
45. European Technical Assessment ETA-12/0062 of 2022/06/01. Available at https://www.dibt.de/pdf_storage/2022/ETA-12!0062(8.06.03-113!22)e.pdf
46. European Committee for Standardization, EN 1382:2016. Timber structures – Test Methods – Withdrawal capacity of timber fastener